Electronic Supplementary Material (ESI) for Polymer Chemistry.

Supplementary Information (SI)

Diazonaphthoquinone-Based Amphiphilic Polymer Assemblies for NIR/UV Light- and pH-Responsive Controlled Release

Qingwei Li, Ziquan Cao, Guojie Wang*

School of Materials Science and Engineering, University of Science and Technology Beijing, Beijing 100083, China

*E-mail: guojie.wang@mater.ustb.edu.cn; Tel: 86-10-62333619

1. ^{1}H NMR spectrum of PEG-PDMAMEMA@DNQ (P2)

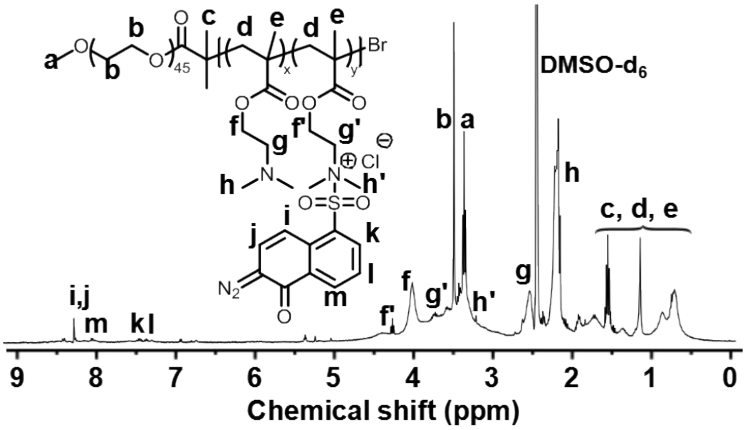

Figure S1. ^{1}H NMR spectrum of PEG-PDMAEMA@DNQ (**P2**) in DMSO-d_6.

2. UV-vis spectra of sc-DNQ, P1 and P2 in DMSO

Figure S2 shows the UV-vis absorbance spectra of 2-diazo-1, 2-naphthoquinone (sc-DNQ, 0.01 mg/mL) and the polymers (**P1** and **P2**, 0.5 mg/mL) in DMSO, from which the molar ratio between DMAEMA and sc-DNQ in **P1** and **P2** could be determined (7.4:1 and 55:1, respectively).

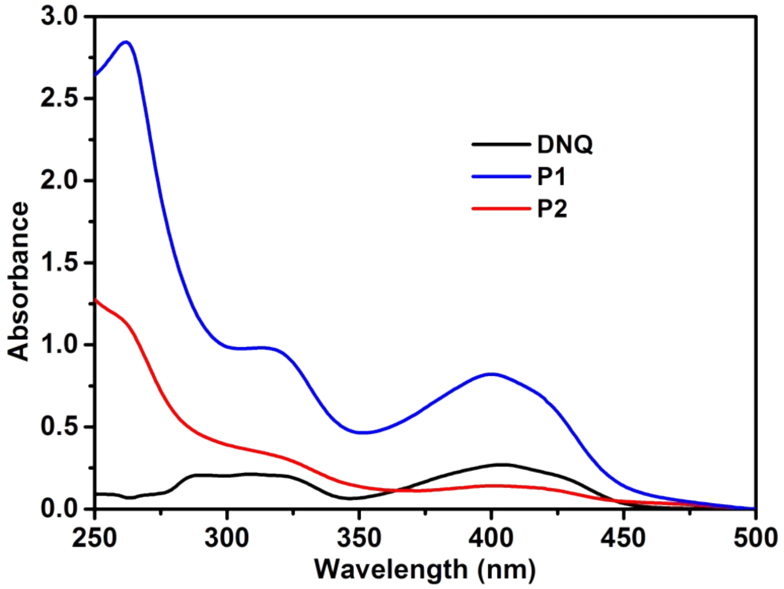

Figure S2. UV-vis absorption spectra of 2-diazo-1, 2-naphthoquinone (sc-DNQ) and the synthesized polymers (**P1** and **P2**) in DMSO.

3. FTIR spectrum of PEG-PDMAEMA@DNQ (P2)

The characteristic vibration peak at around 2200 cm^{-1} assigned to the N≡N of DNQ, a large carbon-nitrogen vibration peak (-N$^+$(CH$_3$)$_2$-) at 3430 cm^{-1} and a carbonyl (C=O) stretch vibration at 1731 cm^{-1} are shown in Figure S3, which proved the quaternization between the amine groups of PEG-PDMAEMA and the chlorine group belongs to DNQ.

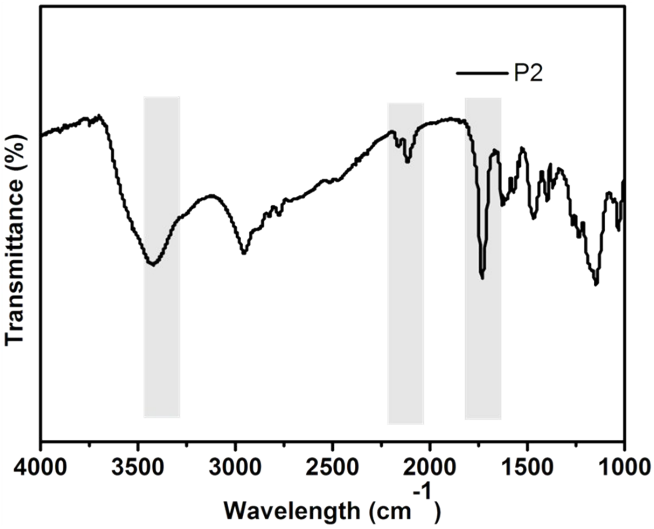

Figure S3. FTIR spectrum of PEG-PDMAEMA@DNQ (**P2**).

4. SEC traces of PEG-PDMAEMA, P1 and P2

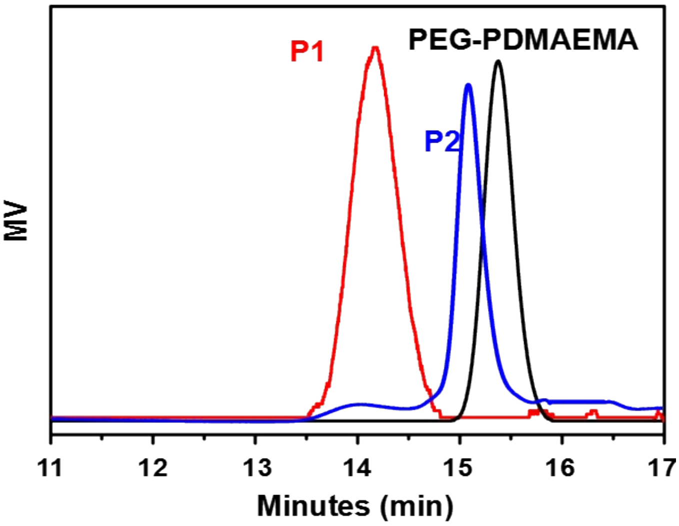

Figure S4. SEC traces of the polymers: PEG-PDMAEMA, **P1** and **P2**

5. Fluorescence emission spectra of coumarin 102 loaded in the polymer assemblies of P1 under pH stimulation for different time

Figure S5 shows the fluorescence emission spectra of coumarin 102 loaded in the polymer assemblies (0.2 mg/mL) at different pH. It can be seen that the characteristic emission intensity of coumarin 102 at about 490 nm progressively decreased with increasing the incubation time, indicating that the coumarin 102 was released from the polymer assemblies under the pH stimulation.

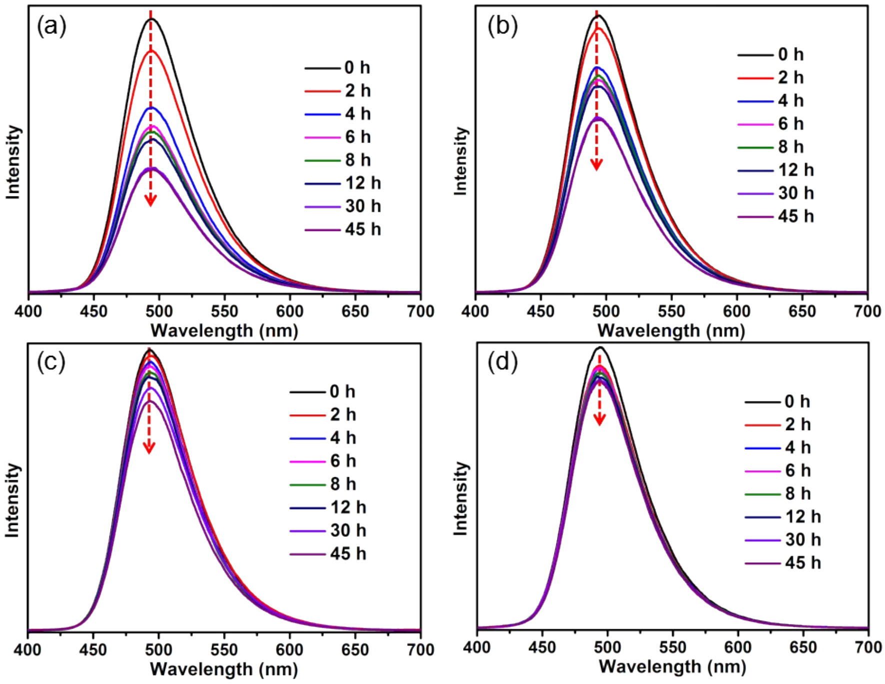

Figure S5. Fluorescence emission spectra of coumarin 102 loaded in the polymer assemblies: (a) at pH 3, (b) at pH 5, (c) at pH 7, (d) at pH 9. λ_{ex}=390 nm.

6. Fluorescence spectra of coumarin 102 loaded in the polymer assemblies of P1 under UV light stimulation at different pH

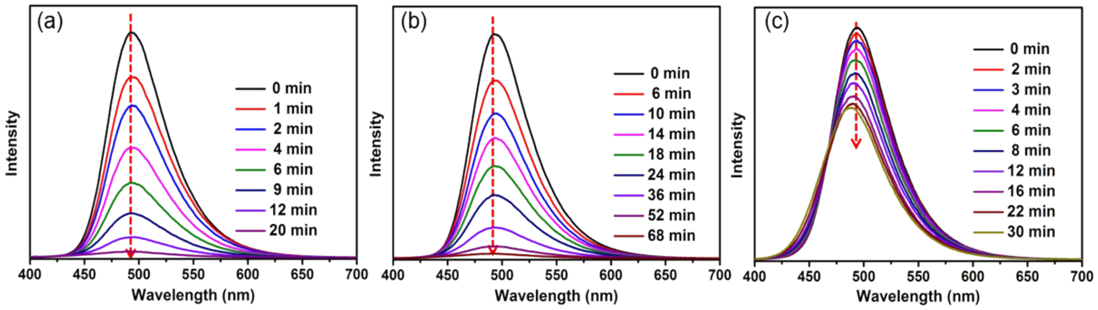

Figure S6. Fluorescence emission spectra of coumarin 102 loaded in the polymer assemblies: (a) under UV light irradiation at pH 3, (b) under UV light irradiation at pH 7, (c) under UV light irradiation at pH 9. The UV light intensity: 40 mW/cm^2; λ_{ex}=390 nm.

7. Fluorescence spectra of coumarin 102 loaded in the polymer assemblies of P1 under NIR light stimulation at different pH

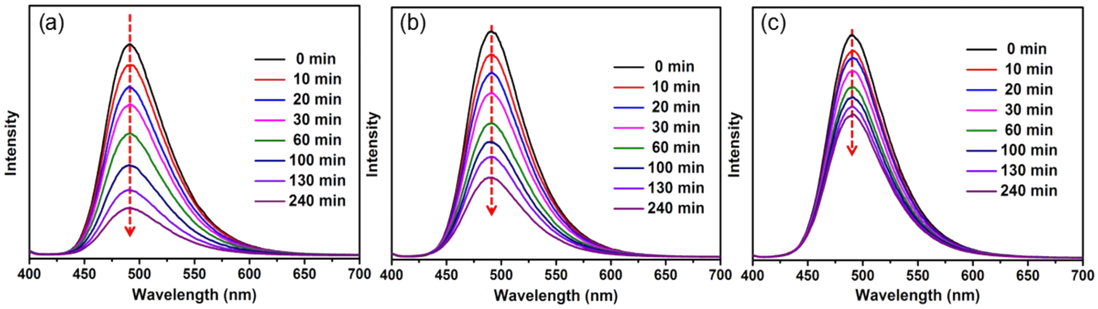

Figure S7. Fluorescence emission spectra of coumarin 102 loaded in the polymer assemblies: (a) under NIR light irradiation at pH 3, (b) under NIR light irradiation at pH 7, (c) under NIR light irradiation at pH 9. The NIR light intensity: 10 W; λ_{ex}=390 nm.

8. Fluorescence intensities of Nile Red with different concentrations

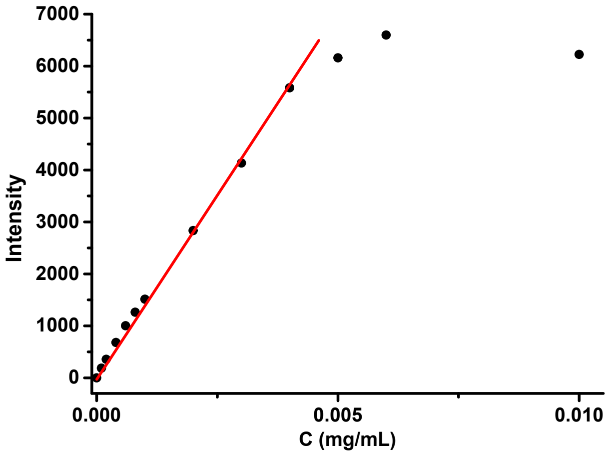

Figure S8. Fluorescence emission intensities of Nile Red at 630 nm vs its concentration in DMF.

Figure S8 shows the relationship between fluorescence intensities of Nile Read and the concentrations. The fluorescence emission intensity increased linearly with the increase of the concentrations at low concentrations, while Nile Red would self-quench themselves at high concentrations. The initial concentrations of Nile Read loaded into the assemblies P1 or P2 were obtained as 0.003 mg/mL and 0.002 mg/mL respectively by using the relationship between the fluorescence intensity and the concentration of Nile Red.

9. Fluorescence intensities of coumarin102 with different concentration

Figure S9 shows that the fluorescence emission intensity at 490 nm increases linearly with the increase of the concentration of courmarin 102 at low concentrations. The initial concentration of coumarin 102 loaded into the assemblies was obtained as 0.0015 mg/mL by using the relationship between the fluorescence intensity and the concentration of coumarin 102.

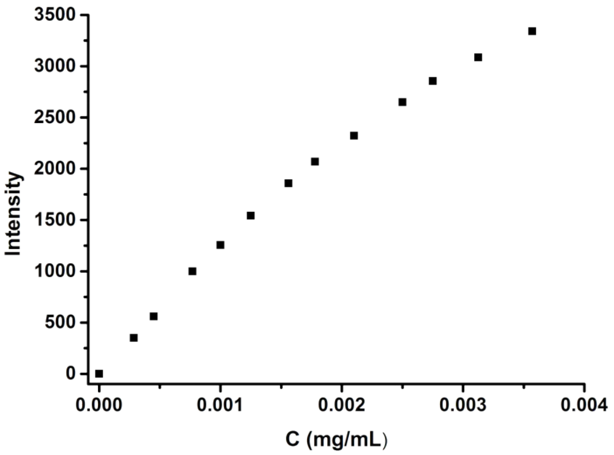

Figure S9. Fluorescence emission intensities of coumarin102 at 490 nm vs concentration for coumarin102 in DMF.

10. Fluorescence spectra of coumarin 102 loaded in the polymer assemblies of P1 under the stimulation of temperature at 60 °C

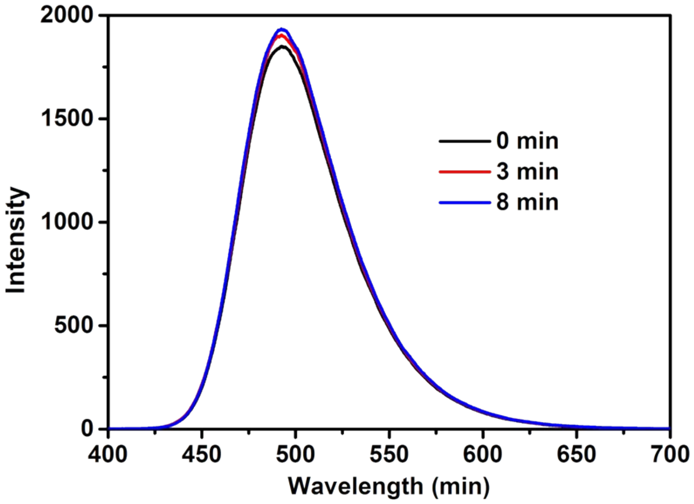

Figure S10. Fluorescence emission spectra of coumarin 102 loaded in the polymer assemblies when heated 60 °C, λ_{ex}=390 nm.

As shown in Figure S10, the fluorescence intensity of coumarin 102 loaded in assemblies changed little when the temperature increased to 60 °C, suggesting the coumarin 102 could not be released, since the PDMAEMA become hydrophobic when the temperature increased to 60 °C (above the LCST), which induced shrinkage of the assemblies.

11. Release profiles of coumarin 102 encapsulated in the polymer assemblies under UV light irradiation with different power densities

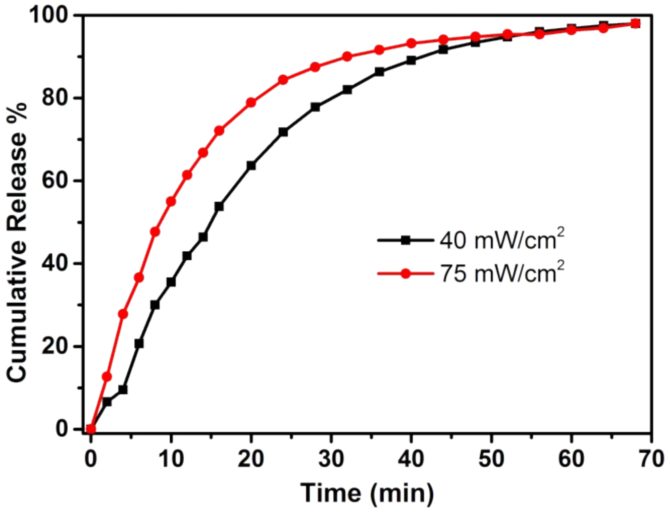

Figure S11. Release profiles of coumarin 102 encapsulated in polymer assemblies under UV light irradiation with different power densities.

12. UV-vis absorption spectra of 2-diazo-1,2-naphthoquinone-5-sulfonyl chloride (DNQ) under different pH

Figure S12 shows the UV-vis absorption spectra of DNQ in DMSO at different pH. When the pH value changed from 7 to 3, the UV-vis absorption spectra changed little. When the pH value changed from 7 to 9, the characteristic absorption peak of DNQ around 400 nm decreased and a new absorption peak at 350 nm appeared due to the formation of napthol via the base catalyzed reaction. Moreover, when the pH of the alkaline solution was adjusted to neutral or acidity, the absorption peak changed little, indicating that the base catalyzed reaction is irreversible.

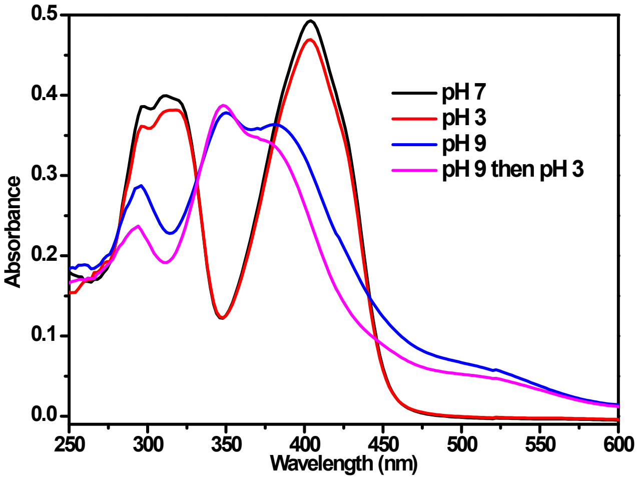

Figure S12. UV-vis absorption spectra of DNQ in DMSO at different pH.